

Noise Shaping Enhanced DMT Signal Transmission Utilizing Low-Resolution DAC

Fan Li¹, Zhibin Luo, Ke Bai¹, Mingzhu Yin, Dongdong Zou¹, Wei Wang, Xiaowu Wang, Wenqin Tan,
Qi Sui, and Zhaohui Li¹

Abstract—In order to reduce the quantization noise of low-resolution DAC, we study a noise shaping technique that can reshape the white quantization noise to an irregular spectrum, in which the noise in the data subcarrier band is almost transformed into the null subcarrier band. Both in simulation and experiment, we verify the effectiveness of the investigated scheme in 25 GHz 16-QAM/32-QAM/64-QAM DMT transmission systems. The experimental results show that the noise shaping technique can enhance the receiver sensitivity of 4-bit quantized 16-QAM DMT and 5-bit quantized 32-QAM DMT by 4.3 dB and 2.5 dB respectively, at BER of hard decision forward error correction (HD-FEC) threshold (3.8×10^{-3}). In addition, with the aid of noise shaping, the performance of 4-bit quantization 16-QAM DMT system is the same as the 8-bit quantization 16-QAM DMT system at the HD-FEC threshold. The experimental results reveal that the proposed noise shaping scheme is a good solution for high-speed, low-cost short reach intra-DCI with low-resolution DAC in future 6G networks evolved from 5G mobile networks.

Index Terms—Noise shaping technique, low-bit resolution system, quantization noise suppression, intra data center interconnects (intra-DCI), intensity modulation and direct detection (IM/DD), discrete multitone (DMT).

I. INTRODUCTION

WITH the explosive emergence of various high bandwidth services, such as cloud services, artificial intelligence

Manuscript received July 28, 2021; revised October 3, 2021; accepted October 9, 2021. Date of publication October 14, 2021; date of current version October 28, 2021. This work was supported in part by the National Key R&D Program of China under Grant 2018YFB1800902, in part by the National Science Foundation of China under Grants U2001601 and 61871408, in part by Local Innovation and Research Teams Project of Guangdong Pearl River Talents Program under Grant 2017BT01X121, in part by the Fundamental and Applied Basic Research Project of Guangzhou City under Grant 202002030326, and in part by the Open Fund of IPOC under Grant IPOC2020A010. (Corresponding author: Fan Li.)

Fan Li, Zhibin Luo, Ke Bai, Mingzhu Yin, Dongdong Zou, Wei Wang, Xiaowu Wang, and Wenqin Tan are with the Guangdong Provincial Key Laboratory of Optoelectronic Information Processing Chips and Systems, School of Electronics and Information Technology, Sun Yat-Sen University, Guangzhou 510275, China (e-mail: lifan39@mail.sysu.edu.cn; luozhb3@mail2.sysu.edu.cn; baik3@mail2.sysu.edu.cn; yinmzh@mail2.sysu.edu.cn; zoudd@mail2.sysu.edu.cn; wangw283@mail2.sysu.edu.cn; wangxw37@mail2.sysu.edu.cn; tanwq25@mail2.sysu.edu.cn).

Qi Sui is with the Guangdong Provincial Key Laboratory of Optoelectronic Information Processing Chips and Systems, Zhuhai 519000, China (e-mail: suiqi@sml-zhuhai.cn).

Zhaohui Li is with the Guangdong Provincial Key Laboratory of Optoelectronic Information Processing Chips and Systems, Sun Yat-sen University, Guangzhou 510275, China, and also with the Southern Marine Science and Engineering Guangdong Laboratory, Zhuhai 519000, China (e-mail: lzh88@mail.sysu.edu.cn).

Digital Object Identifier 10.1109/JPHOT.2021.3119925

(AI) and supercomputing, the requirement for the bandwidth of data center interconnects (DCIs) has been constantly growing [1]–[3]. According to the “Cisco Global Cloud Index: Forecast and Methodology, 2016–2021” [4], the share of machine-to-machine connections will grow from 33 percent in 2018 to 50 percent in 2023, and the internet traffic in intra-DCI occupies 71.5% of the whole traffic generated in DCIs. For the rapid growth of the demand for communication capacity in DCIs, intensity modulation and direct detection (IM/DD) system is a mature architecture to match the capacity requirements. Additionally, advanced modulation formats including quadrature amplitude modulation (QAM) [5]–[7], pulse amplitude modulation (PAM) [8]–[10] and discrete multitone modulation (DMT) [11]–[15] are widely used in offline system demonstration of optical interconnection to achieve high spectral efficiency. Recently, DMT-based IM/DD system [16]–[18] is considered as a promising solution for short reach and high-speed DCIs due to its high spectrum efficiency, high resistance to chromatic dispersion (CD) and simple frequency domain equalization. Although it also suffers from the high peak-to-average power ratio (PAPR) as other multicarrier modulation formats. In addition, to compensate for the bandwidth limitation induced inter-symbol interference (ISI), pre-equalization is usually employed at the transmitter side, however, this will lead to higher PAPR of DMT signal [14]. In this case, signal with high PAPR requires a high-resolution digital-to-analog converter (DAC) to reduce the quantization noise and enhance the signal-to-noise ratio (SNR). However, the evolution of network from 5G towards 6G will need new optical transport architecture with low-cost, low-energy consumption. Especially in short-reach applications such as intra-DCI, in which the fiber transmission distance is less than 2-km [19]–[21], the system cost is the most important concern. The high quantization noise caused by commercial DAC with 4/5/6-bit resolution is an obstacle for high-speed intra-DCI with a high-order modulation format.

To solve this problem, delta-sigma modulation is proposed, in which the noise transfer function is specifically designed to reduce the quantization noise within the signal bandwidth [23]–[29]. The disadvantage is that the delta-sigma modulation requires an ultra-high oversampling rate. A novel noise shaping scheme is proposed in Ref. [30]. Similar to delta-sigma modulation, the operation principle of the noise shaping scheme is to push the quantization noise out of the signal band and increase signal to quantization noise ratio (SQNR), while the required sampling rate is far less than delta-sigma modulation. However,

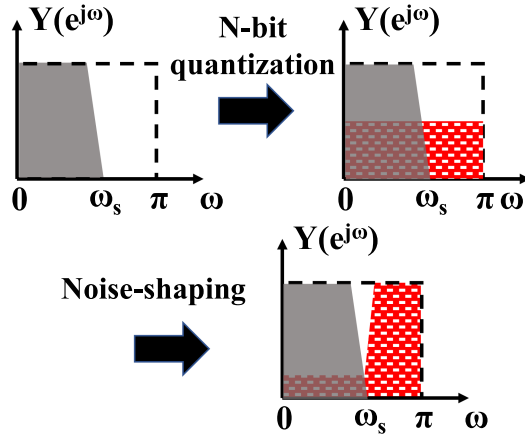


Fig. 1. Operating principle of noise shaping.

Ref. [30] only studies the 5-bit quantization 16-QAM DMT system in simulation, and the interaction between quantization noise and channel noise including the thermal noise from amplifier, shot noise from photodiode (PD) is not considered. Meanwhile, noise shaping technique is also applied to reduce the quantization noise of differential pulse coding modulation (DPCM) in the digital mobile fronthaul [31]. However, the scheme digitizes each DMT signal by time-domain multiplexing, which results in low spectral efficiency. The transmission capacity is not enough to support 100 Gb/s optical interconnection.

This paper is an extension of our previous work reported on OFC 2021 [32], in which only 4/5/6-bit DAC is employed in IM/DD system to verify the impact of noise shaping technique. To further study the noise shaping of DMT signal transmission in optical interconnect, we theoretically analyze the impact of quantization noise and channel noise on the system firstly. In addition, we theoretically analyze and experimentally investigate the performance of the noise shaping technique in the 2-km intra-DCI. The experiment result shows that the noise shaping technique can significantly improve the performance of low-resolution DAC system. With the aid of noise shaping, the performance of 4-bit 16-QAM DMT system is the same as the 8-bit 16-QAM system at the hard decision forward error correction (HD-FEC) threshold, which is a promising low-cost scheme for future 6G networks.

The rest of this paper is organized as follows. Section II presents the principle of noise shaping technique. Section III describes the simulation setup and discussion of results. Section IV illustrates the experimental setup and discussion of results. Finally, our work is summarized in Section V.

II. OPERATION PRINCIPLES

As shown in Fig. 1, the operation principle of noise shaping technique is to reshape the white quantization noise to an irregular spectrum, in which the quantization noise within the signal band is pushed to the higher frequency band without signal. It is noting that high-frequency quantization noise has little effect on the signal band. Thus, only a low oversampling rate is required in this noise shaping scheme. Certainly, the performance gain of the technique increases with the oversampling rate to some extent.

A. Structure of Noise Shaping Technique

Fig. 2(a) illustrates the model of this noise shaping technique, where the $U(z)$, $V(z)$ and $E(z)$ represent the input, output and quantization noise of the N-bit quantizer Q , respectively [30]. The conventional DMT signal is quantized with N bits and the quantization noise can be obtained. After being fed back to the FIR filter, the quantization noise after shaping will be added to the input signal. The purpose is to minimize quantization noise in the signal band. The output $V(z)$ can be expressed as:

$$\begin{aligned} V(z) &= U(z) + (G(z) + 1)E(z) \\ &= U(z) + NTF \times E(z) \end{aligned} \quad (1)$$

where noise transform function (NTF) equals to $G(z) + 1$. Our goal is to select an appropriate $G(z)$ to reconstruct the spectrum of quantization noise so that the power of quantization noise in the $0 \sim \omega_s$ signal band can be compressed less than before this operation, which can be written as

$$\int_{0 \sim \omega_s} |1 + G(e^{j\omega})|^2 P_e(e^{j\omega}) d\omega < \int_{0 \sim \omega_s} P_e(e^{j\omega}) d\omega \quad (2)$$

where $P_e(e^{j\omega})$ is the power spectral density of $e(n)$. Therefore, the optimization problem can be given by

$$\min P_{(0 \sim \omega_s)} = \min \int_{0 \sim \omega_s} |1 + G(e^{j\omega})|^2 d\omega \quad (3)$$

According to Ref. [30], $G(z)$ is implemented by finite impulse response (FIR) filter, as shown in Fig. 2(b) and can be expressed as:

$$G(z) = h_1 z^{-1} + h_2 z^{-2} + \dots + h_n z^{-n} \quad (4)$$

where h_n and n represent the coefficient and tap length, respectively. $G(z)$ can be transformed into frequency domain by the relation of $z = e^{j\omega}$, then the integral problem can be converted to the summation problem. Therefore, the Eq. (3) can be written as:

$$\min P_{(\omega_1, \omega_2, \dots, \omega_s)} = \min_{h_1, h_2, \dots, h_i} \sum_{i=1}^s |1 + H(e^{j\omega_i})|^2 \quad (5)$$

Define the vector \mathbf{K} as:

$$\mathbf{K}_{(\omega_1, \omega_2, \dots, \omega_s)} = \begin{bmatrix} 1 \\ 1 \\ \vdots \\ 1 \end{bmatrix} + \begin{bmatrix} e^{-j\omega_1} & e^{-j2\omega_1} & \dots & e^{-jn\omega_1} \\ e^{-j\omega_2} & e^{-j2\omega_2} & \dots & e^{-jn\omega_2} \\ \vdots & \vdots & \ddots & \vdots \\ e^{-j\omega_s} & e^{-j2\omega_s} & \dots & e^{-jn\omega_s} \end{bmatrix} \begin{bmatrix} h_1 \\ h_2 \\ \vdots \\ h_n \end{bmatrix} \quad (6)$$

$$\text{Defining } E = \begin{bmatrix} e^{-j\omega_1} & e^{-j2\omega_1} & \dots & e^{-jn\omega_1} \\ e^{-j\omega_2} & e^{-j2\omega_2} & \dots & e^{-jn\omega_2} \\ \vdots & \vdots & \ddots & \vdots \\ e^{-j\omega_s} & e^{-j2\omega_s} & \dots & e^{-jn\omega_s} \end{bmatrix}, h = \begin{bmatrix} h_1 \\ h_2 \\ \vdots \\ h_n \end{bmatrix}.$$

Eq. (5) can be written as

$$\min P_{(\omega_1, \omega_2, \dots, \omega_s)} = \min_h \|\mathbf{K}\|_2^2 = \min_h \|1 + Eh\|_2^2 \quad (7)$$

According to Ref. [30], the coefficient h_i of the FIR can be obtained by

$$h = -E^{-1} \times 1 \quad (8)$$

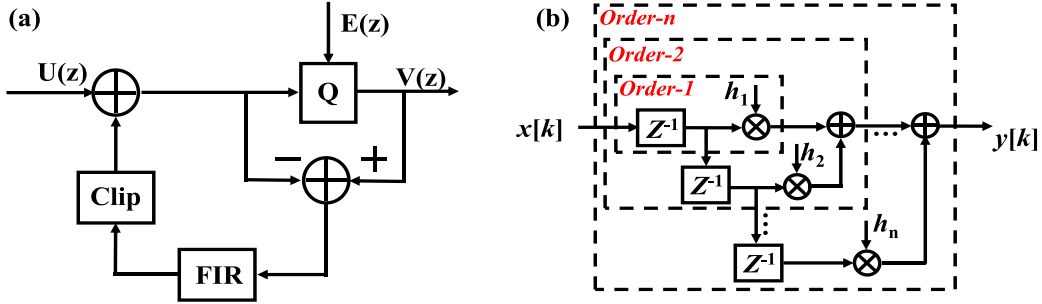


Fig. 2. Linear models of (a) noise shaping technique and (b) FIR filter.

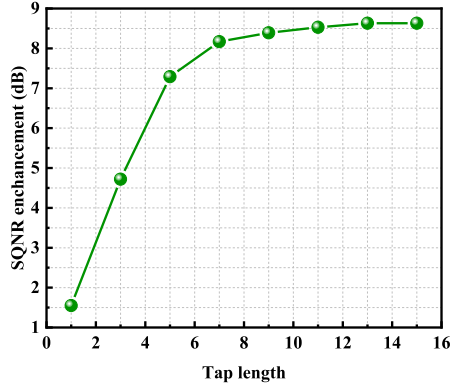


Fig. 3. SQNR enhancement versus Tap length of noise shaping modulator.

where E^{-1} notates the pseudo-inverse of the matrix E . It can be seen that matrix E is determined by the oversampling rate and the FIR tap length n . The key to obtaining the noise transform function is to construct matrix E and calculate the pseudo-inverse of matrix E .

The SQNR enhancement with different tap lengths of FIR is investigated in a 25 GHz QPSK DMT system with 5-bit DAC. The simulation result is shown in Fig. 3. With the increases of the tap length, the enhancement of SQNR is significant until the tap length is equal to 13. Taking both the system performance and computational complexity into consideration, the tap length is fixed at 13 in the following discussion.

It is noteworthy that when the resolution of the quantizer is less than 4 bits, the quantization noise in the feedback loop is too large which will lead to structural overload and instability. In such a situation, a clipper is added to the feedback loop to limit the peak value of $G(z)$ [30]. In contrast, the bit error rate (BER) performance of 5/6/8-bit quantization system is similar with or without a clipper. Considering the complexity of the algorithm, the clipper is only added in the system with less than 4 bits quantization.

B. Performance of Noise Shaping Technique

The effectiveness of noise shaping technique is analyzed theoretically in MATLAB. The 25 GHz QPSK DMT signal is generated with 80 GSa/s sampling rate and quantized with different bits. It means that oversampling rate is 1.6. In addition, the FFT size of the 25 GHz QPSK DMT signal is 1024, the number of payload subcarriers is 640, and the length of cyclic prefix is

12. The SQNR of the quantized DMT signal is calculated with and without noise shaping, as shown in Table I. It exhibits that after noise shaping, the SQNR of 3-bit, 4-bit, 5-bit and 6-bit quantized is improved by 8.5 dB, 8.9 dB, 8.6 dB, and 7.5 dB, respectively.

In a practical IM/DD system, there are channel noises besides quantization noise. To clearly compare quantization noise with channel noise, the SNR of the whole system can be denoted in terms of SQNR and SCNR, which are defined as follows:

$$\text{SQNR} = 10 \times \log_{10} \left(\frac{s^2}{e_q^2} \right) \quad (9)$$

$$\text{SCNR} = 10 \times \log_{10} \left(\frac{s^2}{e_c^2} \right) \quad (10)$$

where s represents signal, e_q and e_c represent quantization noise and channel noises, respectively.

$$\text{SNR} = 10 \times \log_{10} (s^2 / (e_c^2 + e_q^2)) \quad (11)$$

The SNR of the whole system can be written as

Substituting Eq. (9) and Eq. (10) into Eq. (11), SNR can be given by:

$$\text{SNR} = \text{SCNR} - 10 \times \log_{10} \left(1 + 10^{\left(\frac{\text{SCNR}-\text{SQNR}}{10} \right)} \right) \quad (12)$$

In additive white Gaussian noise (AWGN) channel, the relationship between BER and SNR can be expressed as [33]:

$$\text{BER} \cong \frac{\sqrt{M} - 1}{\sqrt{M} \log_2 \sqrt{M}} \text{erfc} \left[\sqrt{\frac{3 \log_2 M \times E_b N_o}{2(M-1)}} \right] \quad (13)$$

where M is modulation order, $E_b N_o$ denotes the SNR per bit and can be expressed as:

$$E_b N_o = \text{SNR} \times \left(\frac{B W}{R_b} \right) \quad (14)$$

where BW is signal bandwidth, R_b is the bit rate

$$R_b = R_s \times \log_2 M \quad (15)$$

where R_s is the sampling rate. According to Eq. (9), the SQNR of an 8-bit quantized DMT signal is about 40 dB. Meanwhile, the SNR of 25 GHz DMT system with 8-bit resolution is investigated at the received optical power (ROP) of 3 dBm, as shown in Fig. 4(a). The calculated average SNR is 21 dB, so according to Eq. (12), the optimal SCNR of this experimental system is about

TABLE I
SQNR WITH DIFFERENT QUANTIZATION BIT AND QUANTIZATION METHOD

Quantization bit	3		4		5		6	
Quantization Method	w/ NS	w/o NS						
SQNR (dB)	20.3	11.8	27.7	18.8	33	24.4	37.9	30.4

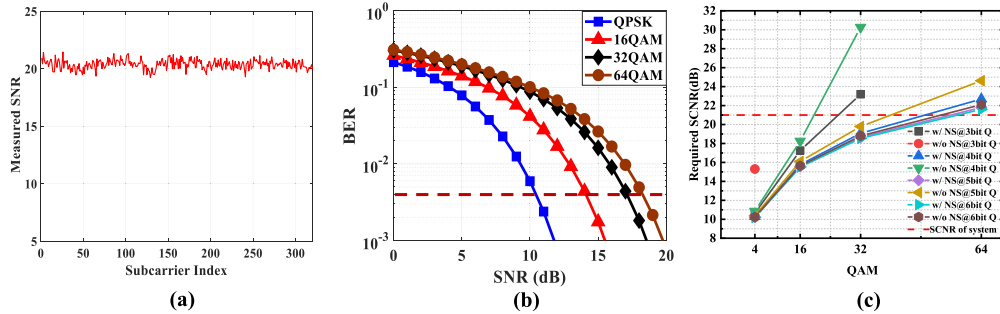


Fig. 4. (a) Measure SNR of pre-equalized signal. (b) BER vs. SNR curves of M-QAM. (c) Required SCNR vs. QAM curves at HD-FEC threshold.

21 dB which is used as the SCNR threshold of the experiment system in the subsequent discussion.

According to Eq. (13)–(15), the BER versus SNR of 25 GHz DMT signal with QPSK/16-QAM/32-QAM/64-QAM is shown in Fig. 4(b). It indicates that when the BER of QPSK/16-QAM/32-QAM/64-QAM signal reaches the HD-FEC (3.8×10^{-3}), the theoretically required SNR is 10.2 dB, 14.2 dB, 16.3 dB and 18.4 dB, respectively. However, nonlinear effects within key components including electrical amplifier and electrical-to-optical (E/O) modulator may introduce penalty to the high-order modulation format signal, so the required SNR in experimental system is 10.2 dB, 15.5 dB, 18.5 dB and 21.5 dB, respectively. Therefore, according to Table I and Eq. (12), the required SCNR for different modulation format signals with and without noise shaping to reach HD-FEC threshold in different quantization systems is calculated, as shown in Fig. 4(c). It indicates that for 3-bit quantization system without noise shaping, the quantization noise is too large to support the 16-QAM/32-QAM/64-QAM signal to reach HD-FEC threshold. In contrast, the required SCNR for the 16-QAM DMT signal with noise shaping to reach HD-FEC threshold in the 3-bit quantization system is 17.3 dB, which is lower than the SCNR threshold denoted by a red line. As for the 4-bit quantization system, it can support the 32-QAM signal to reach HD-FEC threshold with noise shaping. For a 5-bit system, with the help of noise shaping technique, its performance is similar to the 6-bit quantization system. Additionally, the BER of the 64-QAM DMT signal with 4/5/6-bit quantization will not reach below the HD-FEC threshold since the channel noise of the experiment system is too large.

III. SIMULATION SETUP AND RESULTS

A. Simulation Setup

Fig. 5 shows the simulation setup of DMT-based IM/DD system carried out by VPI-transmissionMaker 9.5 and MATLAB.

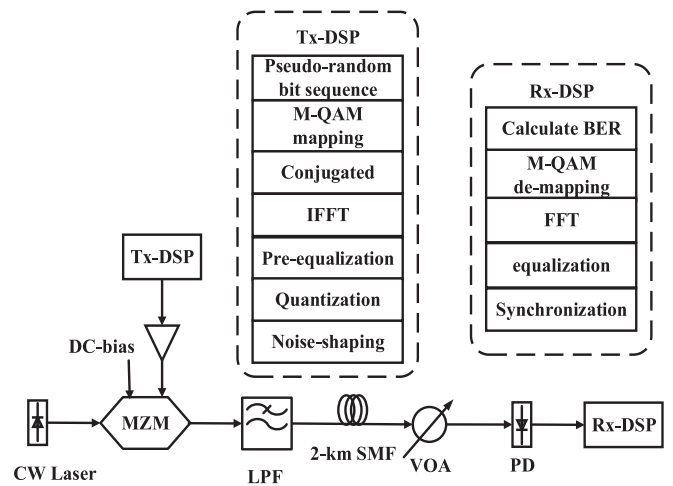


Fig. 5. Simulation setup. Insets are the DSP blocks of the DMT transceiver.

The key parameters are given out in Table II. The insets of Fig. 5 are the DSP blocks of the DMT transceiver. In the transmitter, the pseudo-random bit sequence (PRBS) is mapped into M-QAM and then 25 GHz DMT signal is generated. The FFT size, the number of payload subcarriers and the length of CP are the same as in Section II-B. Besides, each frame has 2 training sequences (TSs) and 251 data-carrying DMT symbols. The pre-equalization is adopted to improve performance. Then, noise shaping is performed after N-bit quantization. At the receiver end, channel equalization is carried out based on the TSs after synchronization. Finally, it is followed by M-QAM de-mapping and BER counting.

B. Simulation Results

The BER performance of the optical interconnects system with different DAC resolutions and modulation formats is investigated in the simulation and shown in Fig. 6. As shown in Fig. 6(a), the receiver sensitivity of QPSK signal in the 3-bit

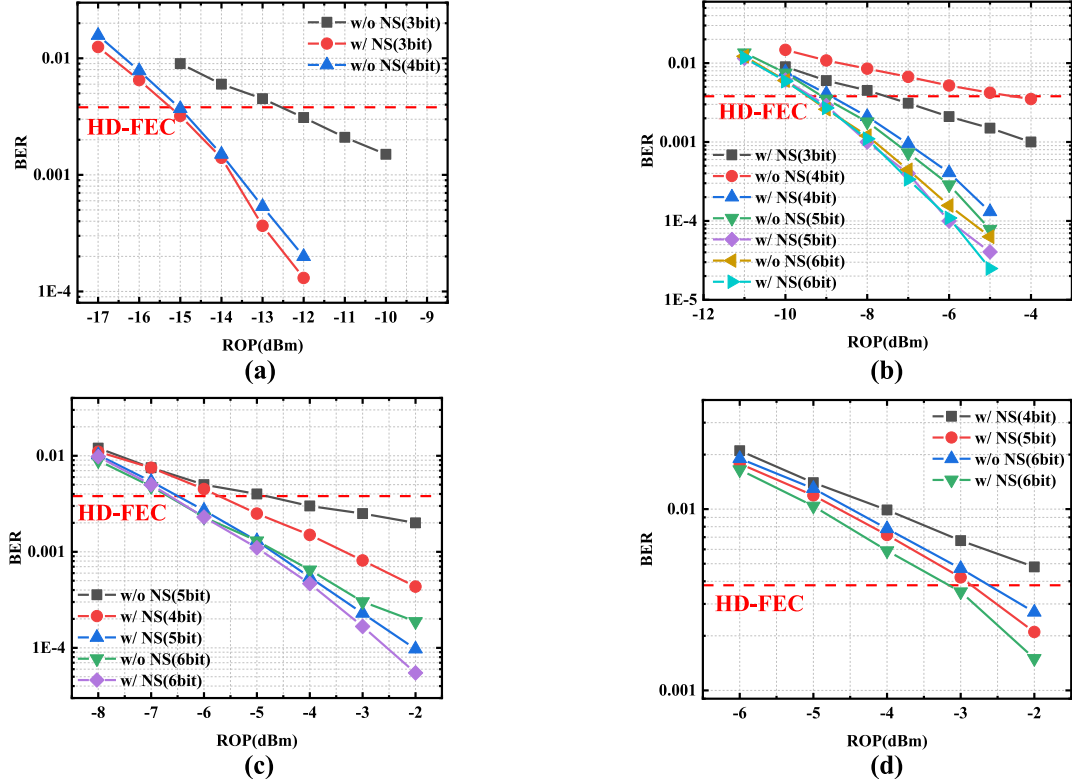


Fig. 6. Simulation results of BER versus ROP of the DMT signal modulated by (a) QPSK, (b) 16-QAM, (c) 32-QAM, and (d) 64-QAM.

TABLE II
KEY PARAMETERS IN SIMULATION SETUP

Parameter	Value
DAC sampling rate	80 Gsa/s
ECL linewidth	100 kHz
ECL wavelength	1552.52 nm
ECL average power	1×10^{-3} W
V _{pi} RF	5 V
V _{pi} DC	5 V
Fiber length	2 km
Attenuation coefficient	0.2 dB/km
Dispersion	16ps/nm/km
Dispersion slope	0.08ps/nm ² /km
Core area	80 μm^2
Nonlinear index	2.6×10^{-20}
Noise power density	1×10^{-15} W/Hz
PD responsivity	1 A/W
PD bandwidth	40 GHz
PD thermal noise	10 pA/Hz ^{0.5}

quantization system is improved by 3 dB with the help of noise shaping technique, and its performance is slightly better than the 4-bit quantization system. Fig. 6(b) shows the BER versus ROP of the 16-QAM DMT signal with and without noise shaping. It is verified that the 3-bit quantization system can transmit 16-QAM DMT signal under the HD-FEC threshold with the help of noise shaping, and it outperforms the 4-bit quantization system without noise shaping. Additionally, the noise shaping technique reduced the ROP from -4.6 dBm to -8.9 dBm at the HD-FEC threshold.

For 32-QAM DMT signal, under the effect of noise shaping, the ROP of 4-bit quantization system is 1 dB lower than the

5-bit quantization system without noise shaping at the HD-FEC threshold. At the same time, the performance of 5-bit quantization system with noise shaping is similar to the 6-bit quantization system as shown in Fig. 6(c). The performance of 64-QAM DMT signal is also simulated and shown in Fig. 6(d). When the ROP is lower than -3.5 dBm, the SCNR is lower than 21 dB, and the 6-bit quantization system will not support the transmission of 64-QAM DMT signal, which verifies the analysis in Section II-B above.

To sum up, the noise shaping technique can significantly improve the performance of low-resolution DAC system. The simulation results show that when the BERs of QPSK DMT, 16-QAM DMT and 32-QAM DMT signal reach the HD-FEC threshold, the minimum quantization bits are 3 bits, 4 bits and 5 bits respectively. In addition, the experiments will be carried out to further verify the effectiveness of noise-shaping technique in the intra-DCI.

IV. EXPERIMENTAL SETUP AND RESULTS

A. Experimental Setup

The experimental setup is presented in Fig. 7. By using the same DSP algorithm as the simulation, the 25 GHz DMT signal is generated offline by MATLAB. The electrical spectra before and after noise shaping are shown in Fig. 7(a) and (b), respectively. The net rate of 16-QAM/32-QAM/64-QAM DMT signal is approximately 91.65/113.99/137.47 Gb/s, excluding 7% FEC overhead. Finally, the signal is uploaded into a Fujitsu DAC with a sampling rate of 80 GSa/s and a 3-dB bandwidth of

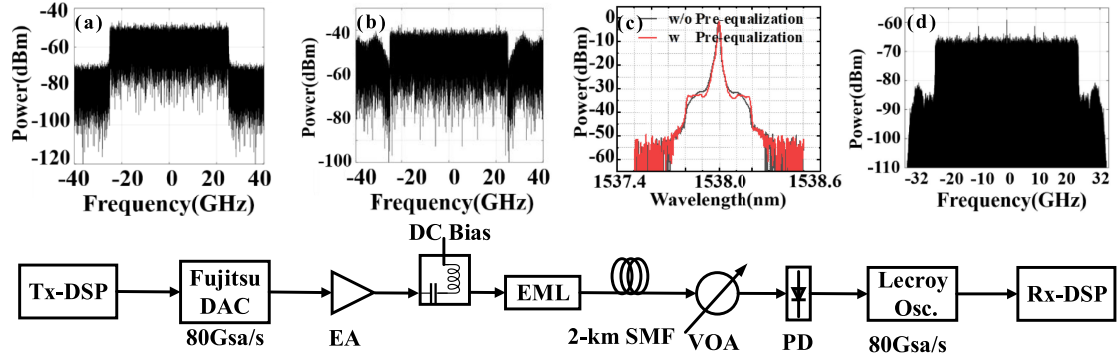


Fig. 7. Experimental setup. (a) Electronic spectrum of quantized signal. (b) Electronic spectrum of signal modulated by noise shaping modulation. (c) Optical spectrum of transmitted signal. (d) Electronic spectrum of received signal.

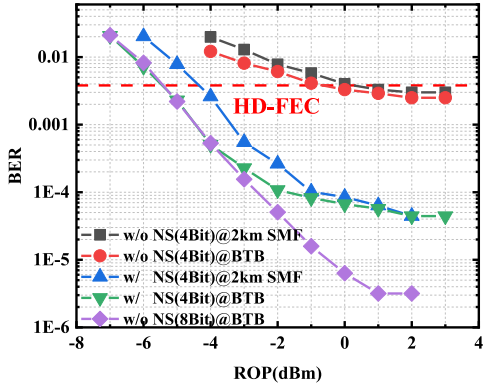


Fig. 8. Experimental measured BER versus ROP curves of 16-QAM DMT.

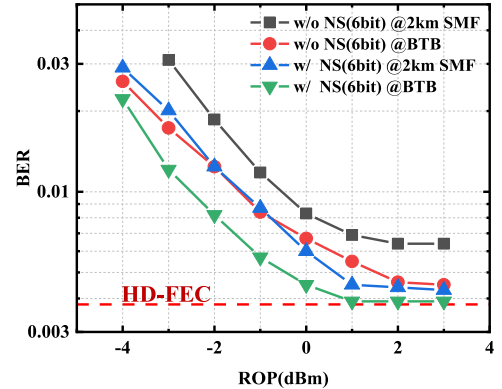


Fig. 10. Experimental measured BER versus ROP curves of 64-QAM DMT.

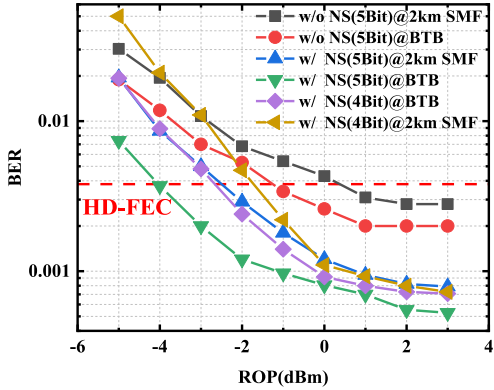


Fig. 9. Experimental measured BER versus ROP curves of 32-QAM DMT.

16.7 GHz, and boosted by a 30 GHz electrical amplifier (EA) with 20 dB gain. Before E/O conversion, a bias-tee is applied for direct current (DC) coupling. A 32 GHz OKI OL5157M electro-absorption modulated laser (EML) is used to achieve E/O conversion with an output power of 5 dBm at 1538 nm. And the optical spectrum of signal with and without pre-equalization is shown in Fig. 7(c). After 2-km single mode fiber (SMF) transmission, a variable optical attenuator (VOA) is used to adjust the ROP, and the signal is detected by a single-ended PD. The signal captured by an oscilloscope with a sampling

rate of 80 GSa/s is processed offline in MATLAB. Since the pre-equalization is only applied in the signal band, the power of the received data subcarrier band is much higher than the power of the null subcarrier band, as shown in Fig. 7(d).

B. Experimental Results

In the experiment, we demonstrate the transmission and reception of 25 GHz DMT signal generated by 4/5/6-bit resolution DAC in the 2-km SMF intra-DCI with and without noise shaping technique. Fig. 8 gives out the measured BER performance versus the ROP of 16-QAM DMT signal. It indicates that the receiver sensitivity of the 4-bit quantization system is improved by 4.3 dB with the help of noise shaping technique, and its BER performance is the same as the 8-bit quantization system without noise shaping when the ROP is less than -4 dBm. However, 8-bit quantization system outperforms 4-bit quantization system with noise shaping technique at higher ROP. This is because quantization noise dominates the performance of system when the channel noise is negligible. After 2-km SMF transmission, 1 dB ROP sensitivity penalty at HD-FEC threshold can be observed for 4-bit quantization system with noise shaping technique.

As shown in Fig. 9, the receiver sensitivity of the 5-bit quantization 32-QAM DMT system is improved by 2.5 dB after 2-km SMF transmission with noise shaping technique. 4-bit quantization system with noise shaping technique can also

support transmission of 32-QAM DMT, and it shows 1.4 dB ROP sensitivity improvement compared with 5-bit quantization system without noise shaping.

For 64-QAM DMT signal, the 6-bit quantization system with noise shaping achieves 1 dB ROP sensitivity improvement compared with the 6-bit system without noise shaping, as shown in Fig. 10. At the same time, it verifies the above discussion that the channel noise of the experimental system is too large to support such 64-QAM modulation format at the HD-FEC threshold. Based on the above discussion, it is concluded that the experimental results are consistent with the simulation results.

V. CONCLUSION

In this paper, it is the first time to experimentally demonstrated the transmission of DMT signal generated by 4/5/6-bit resolution DAC with noise shaping technique in beyond 100 Gb/s intra-DCI to the best of our knowledge. The effect of quantization noise and channel noise on the system are analyzed theoretically. The impact of noise shaping technique is investigated in simulation and experiment. With the help of noise shaping, the receiver sensitivity of 4-bit quantization 16-QAM DMT and 5-bit quantization 32-QAM DMT at HD-FEC threshold can be improved by 4.3 dB and 2.5 dB, respectively. In addition, the receiver sensitivity of 4-bit quantization 16-QAM system with noise shaping is improved by 4.3 dB, and its BER performance is the same as the 8-bit quantization system without noise shaping at HD-FEC threshold. Noise shaping enabled signal transmission utilizing low-resolution DAC is a practical low-cost inter-DCI solution for future 6G mobile networks.

REFERENCES

- [1] F. Li, X. Li, J. Zhang, and J. Yu, "Transmission of 100-Gb/s VSB DFT-Spread DMT signal in short-reach optical communication systems," *IEEE Photon. J.*, vol. 7, no. 5, Oct. 2015, Art. no. 7904307.
- [2] Z. Li, I. Shubin, and X. Zhou, "Optical interconnects: Recent advances and future challenges," *Opt. Exp.*, vol. 23, no. 3, pp. 3717–3720, 2015.
- [3] W.-R. Peng, I. Morita, H. Takahashi, and T. Tsuritani, "Transmission of high-speed (>100 Gb/s) direct-detection optical OFDM super channel," *J. Lightw. Technol.*, vol. 30, pp. 2025–2034, 2012.
- [4] Cisco visual networking index: Forecast and methodology 2016–2021, San Jose, CA, USA, 2016. [Online] Available: <https://www.reinvention.be/webhdfs/v1/docs/complete-white-paper-c11-481360.pdf>
- [5] A. S. Karar and J. C. Cartledge, "Generation and detection of a 112-Gb/s dual polarization signal using a directly modulated laser and half-cycle 16-QAM Nyquist-subcarrier-modulation," in *Proc. Eur. Conf. Exhib. Opt. Commun.*, 2012, Art. no. Th.3. A.4.
- [6] Z. Xing *et al.*, "100 Gb/s 16-QAM transmission over 80 km SSMF using a silicon photonic modulator enabled VSB-IM/DD system," in *Proc. Conf. Opt. Fiber Commun.*, 2018, Art. no. M2C.7.
- [7] R. T. Kamurthi, S. R. Chopra, and A. Gupta, "Higher order QAM schemes in 5G UFMC system," in *Proc. Emerg. Smart Comput. Inform.*, 2020, pp. 198–202.
- [8] F. Li *et al.*, "200 Gbit/s (68.25 gbaud) PAM8 signal transmission and reception for intra-data center interconnect," in *Proc. Conf. Opt. Fiber Commun.*, 2019, Art. no. W4I.3.
- [9] Y. Fu *et al.*, "Computationally efficient 120 Gb/s/λ PWL equalized 2D-TCM-PAM8 in dispersion unmanaged DML-DD system," in *Proc. Conf. Opt. Fiber Commun.*, 2018, Art. no. We1H.5.
- [10] F. Li *et al.*, "100 Gbit/s PAM4 signal transmission and reception for 2-km interconnect with adaptive notch filter for narrowband interference," *Opt. Exp.*, vol. 26, no. 18, pp. 24066–24074, 2018.
- [11] C. Xie *et al.*, "Single-VCSEL 100-Gb/s short-reach system using discrete multi-tone modulation and direct detection," in *Proc. Conf. Opt. Fiber Commun.*, 2015, Art. no. Tu2H.2.
- [12] F. Li *et al.*, "Demonstration of four-channel CWDM 560 Gbit/s 128QAM-OFDM for optical inter-connection," in *Proc. Conf. Opt. Fiber Commun.*, 2016, Art. no. W4J.2.
- [13] B. Yu *et al.*, "150-Gb/s SEFDM IM/DD transmission using log-MAP viterbi decoding for short reach optical links," *Opt. Exp.*, vol. 26, no. 24, pp. 31075–31084, 2018.
- [14] D. Zou *et al.*, "Comparison of bit-loading DMT and pre-equalized DFT-spread DMT for 2-km optical interconnect system," *J. Lightw. Technol.*, vol. 37, no. 10, pp. 2194–2200, May 2019.
- [15] L. Zhang, J. V. Kerrebrouck, R. Lin, X. Pang, A. Udalcovs, and X. Yin, "Nonlinearity tolerant high-speed DMT transmission with 1.5-μm single-mode VCSEL and multi-core fibers for optical interconnects," *J. Lightw. Technol.*, vol. 37, no. 2, pp. 380–388, 2019.
- [16] K. Zhong *et al.*, "Experimental study of PAM-4, CAP-16, and DMT for 100 Gb/s short reach optical transmission systems," *Opt. Exp.*, vol. 23, no. 2, pp. 1176–1189, 2015.
- [17] L. Nadal *et al.*, "DMT modulation with adaptive loading for high bit rate transmission over directly detected optical channels," *J. Lightw. Technol.*, vol. 32, no. 21, pp. 4143–4153, Nov. 2014.
- [18] P. Dong *et al.*, "Four-channel 100-Gb/s per channel discrete multitone modulation using silicon photonic integrated circuits," *J. Lightw. Technol.*, vol. 34, no. 1, pp. 79–84, Jan. 2016.
- [19] D. Zou, Z. Li, Y. Sun, F. Li, and Z. Li, "Computational complexity comparison of single-carrier DMT and conventional DMT in data center interconnect," *Opt. Exp.*, vol. 27, no. 12, pp. 17007–17016, 2019.
- [20] A. Dochhan, N. Eiselt, J. Zou, H. Griesser, M. H. Eiselt, and J. Elbers, "Real-time 112 Gbit/s DMT for data center interconnects," in *Proc. Int. Conf. Photon.*, 2018, Art. no. SpTh4F.3.
- [21] D. Zou *et al.*, "Comparison of null-subcarriers reservation and adaptive notch filter for narrowband interference cancellation in intra-data center interconnect with DMT signal transmission," *Opt. Exp.*, vol. 27, no. 4, pp. 5696–5702, 2019.
- [22] J. Wang *et al.*, "Delta-Sigma modulation for digital mobile fronthaul enabling carrier aggregation of 32 4G-LTE /30 5G-FBMC signals in a Single-λ 10-Gb/s IM/DD channel," in *Proc. Conf. Opt. Fiber Commun.*, 2016, Art. no. W1H.2.
- [23] H. Li *et al.*, "Improving performance of mobile fronthaul architecture employing high order delta-sigma modulator with PAM-4 format," *Opt. Exp.*, vol. 25, no. 1, pp. 1–9, 2017.
- [24] J. Wang, Z. Jia, L. Campos, L. Cheng, C. Knittle, and G. Chang, "Delta-Sigma digitization and optical coherent transmission of DOCSIS 3.1 signals in hybrid fiber coax networks," *J. Lightw. Technol.*, vol. 36, no. 2, pp. 568–579, Jan. 2018.
- [25] H. Li *et al.*, "A 21-GS/s single-bit second-order delta-sigma modulator for FPGAs," *IEEE Trans. Circuits Syst., II, Exp. Briefs*, vol. 66, no. 3, pp. 482–486, Mar. 2019.
- [26] C. Wu *et al.*, "Distributed multi-user MIMO transmission using real-time sigma-delta-over-fiber for next generation fronthaul interface," *J. Lightw. Technol.*, vol. 38, no. 4, pp. 705–713, Feb. 2020.
- [27] J. Wang, Z. Jia, L. A. Campos, and C. Knittle, "Delta-Sigma modulation for next generation fronthaul interface," *J. Lightw. Technol.*, vol. 37, no. 12, pp. 2838–2850, Jun. 2019.
- [28] R. Schreier, *Understanding Delta Sigma Data Converters*. 2nd ed., Oregon State, USA: Wiley, 2004.
- [29] R. Gray, "Oversampled sigma delta modulation," *IEEE Trans. Commun.*, vol. COM-35, no. 5, pp. 481–489, May 1987.
- [30] W. A. Ling, "Shaping quantization noise and clipping distortion in direct-detection discrete multitone," *J. Lightw. Technol.*, vol. 32, no. 9, pp. 1750–1758, May 2014.
- [31] H. Li, X. Li, and M. Luo, "Improving performance of differential pulse coding modulation based digital mobile fronthaul employing noise shaping," *Opt. Exp.*, vol. 26, no. 9, pp. 11407–11417, 2018.
- [32] K. Bai *et al.*, "Quantization noise suppression with noise shaping technique in DMT-modulated IM/DD optical interconnects utilizing low-resolution DAC," in *Proc. Conf. Opt. Fiber Commun.*, 2021, Art. no. W6A.19.
- [33] K. Cho and D. Yoon, "On the general BER expression of one- and two-dimensional amplitude modulations," *IEEE Trans. Commun.*, vol. 50, no. 7, pp. 1074–1080, Jul. 2002.